Chlorophylls and Bacteriochlorophylls: Biochemistry, Biophysics, Functions and Applications
B. Grimm, R. Porra, W. Rüdiger, H. Scheer (eds.)

Vol. 25 of Advances in Photosynthesis and Respiration
Govindjee (series editor)

Published 2006 by Springer, ISBN 1-4020-4515-8

Supplement to chapter 30
Mechanisms of Carotenoid-to-Bacteriochlorophyll Energy Transfer in the Light Harvesting Antenna Complexes 1 and 2 (Y. Koyama, Y. Kakitani)

Mechanisms of Carotenoid-to-Bacteriochlorophyll Energy Transfer in the Light Harvesting Antenna Complexes 1 and 2: Dependence on the Conjugation Length of Carotenoids

Yasushi Koyama* and Yoshinori Kakitani

Faculty of Science and Technology, Kwansei Gakuin University,

2-1 Gakuen, Sanda, Hyogo 669-1337, Japan

*Correspondence:

Prof. Yasushi Koyama

Faculty of Science and Technology, Kwansei Gakuin University, 2-1 Gakuen, Sanda, Hyogo 669-1337, Japan

Phone: +81-79-565-8408 Fax: +81-79-565-9077 E-mail: ykoyama@kwansei.ac.jp

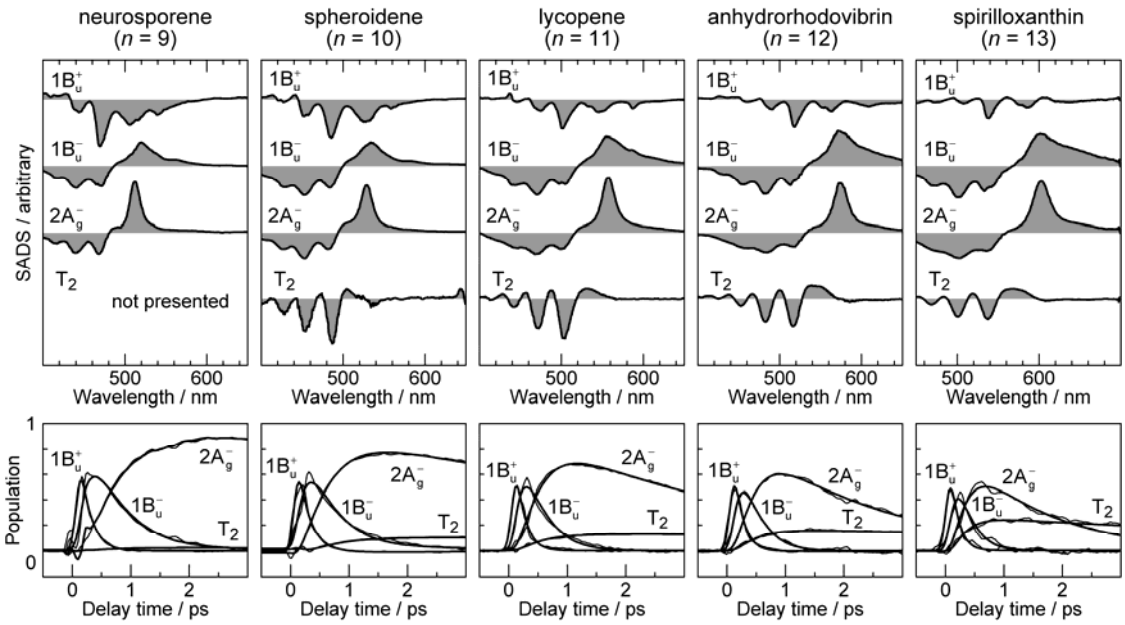

Fig. S1. The SADS (the top panels) and the time-dependent changes in population (the bottom panels) for the $1B_u^+$, $1B_u^-$ and $2A_g^-$ singlet-excited states and the T_2 ($1A_g$) state, that were obtained by the SVD and global-fitting analyses of the visible, subpicosecond time-resolved spectra of neurosporene (n = 9), spheroidene (n = 10), lycopene (n = 11), anhydrorhodovibrin (n = 12) and spirilloxanthin (n = 13) in the visible region (see Fig. 3 for the relaxation scheme).

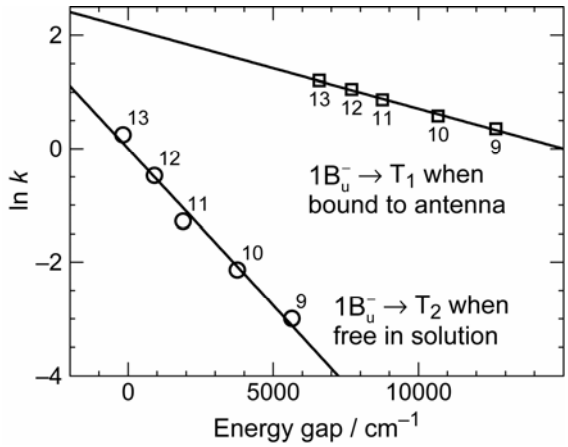

Fig. S2. The rates of the $1B_u^- \rightarrow T_2$ singlet-to-triplet electronic conversion in solution and those of the $1B_u^- \rightarrow T_1$ singlet-to-triplet electronic conversion in the LH1 complexes fitted to an approximate energy-gap law in the form $\ln k = A - B \times \Delta E$, where k and ΔE are the rate (in ps^{-1}) and the energy gap (in cm^{-1}), respectively. $A = 2.0 \times 10^{-3}$ and $B = 5.5 \times 10^{-4}$ cm in solution, and $A = 2.1$ and $B = 1.4 \times 10^{-4}$ cm in LH1. The number of the conjugated double bonds, n, is indicated for each Car.

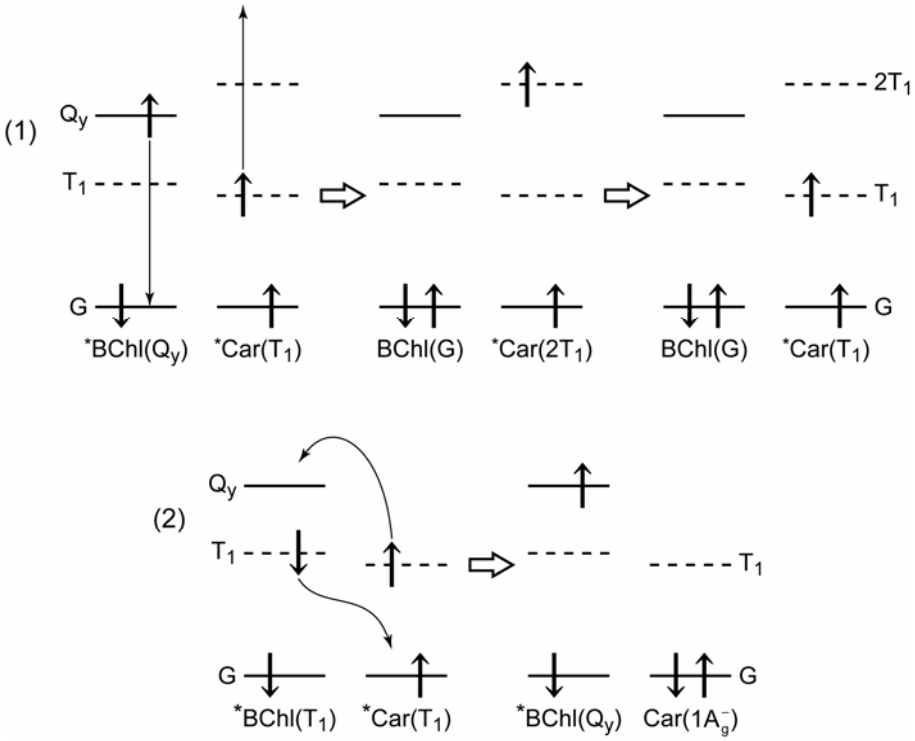

Fig. S3. The detailed mechanisms of the excited-state reactions shown in Eqs. 1 and 2 in the text. They include (1) BChl-Car singlet-triplet annihilation and, (2) BChl-Car triplet-triplet annihilation to generate the Q_y state of BChl. Asterisks indicate the excited states.

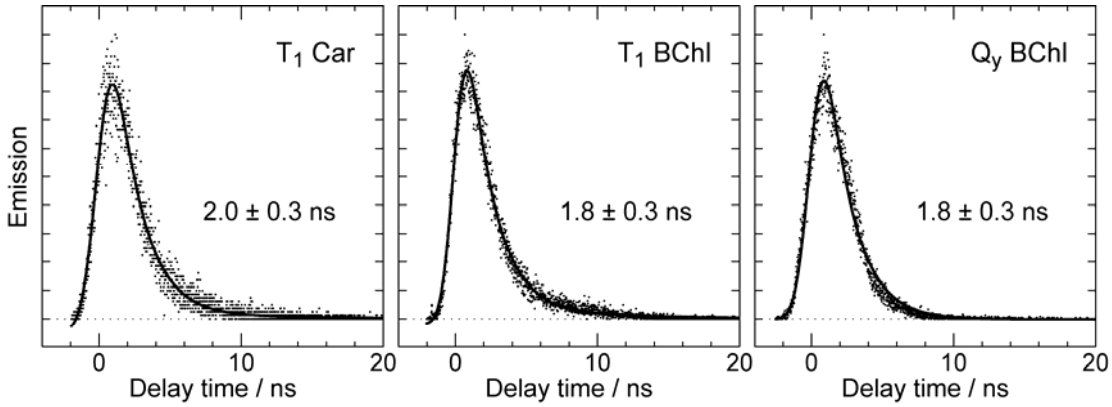

Fig. S4. Time profiles for T_1 Car, T_1 BChl and Q_y BChl in the LH2 complex from *Rba. sphaeroides* G1C determined by phosphorescence spectroscopy. The decay time constants are indicated in each panel.

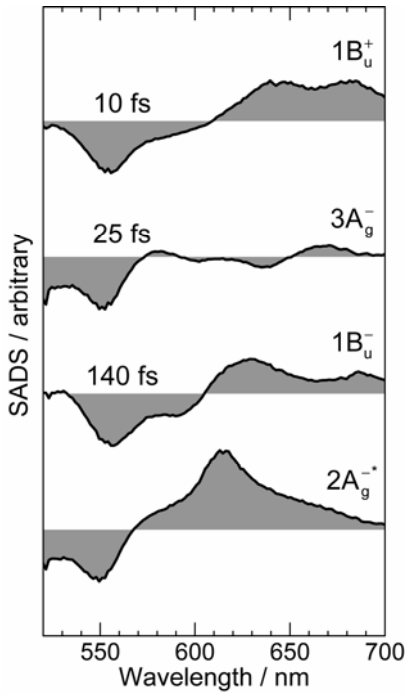

Fig. S5. The SADS for the $1B_u^+$, $3A_g^-$, $1B_u^-$ and $2A_g^-$ states of spirilloxanthin (n = 13) as the result of the SVD and global-fitting analysis of the time-resolved spectral data matrix that were obtained by the use of 5 fs pump-and-probe pulses. (Nishimura K, Rondonuwu FS, Fujii R, Akahane J, Koyama Y and Kobayashi T (2004) Sequential singlet internal conversion of $1B_u^+ \rightarrow 3A_g^- \rightarrow 1B_u^- \rightarrow 2A_g^- \rightarrow (1A_g^-$ ground) in all-*trans*-spirilloxanthin revealed by two-dimensional sub-5-fs spectroscopy. Chem Phys Lett 392: 68–73)